A High-Performance Wastewater Treatment System for Orange II Degradation Using a Boron-doped Diamond Electrode and Enhanced by Zeolite-TiO$_2$ Photocatalyst

Daibing Luo[1,2], Daichuan Ma[1], Liangzhuan Wu[2,*] Jinfang Zhi[2,*]

[1] Analytical & Testing Center, Sichuan University, No.29, Wangjiang Road, Wuhou District, Chengdu, 610064, China
[2] Key Laboratory of Photochemical Conversion and Optoelectronic Materials, Technical Institute of Physics and Chemistry, Chinese Academy of Sciences, Beijing 100190, China;
[*]E-mail: Wuliangzhuan@mail.ipc.ac.cn; zhi-mail@mail.ipc.ac.cn

A wastewater treatment system has been studied which is composed of an electrochemical cell and a photocatalysis unit. A boron-doped diamond (BDD) electrode and TiO$_2$-loaded zeolite (zeolite-TiO$_2$) were used in the electro-photo process, and the joint treatment efficiency was assessed Orange II degradation. The photo-electro treatment of Orange II in aqueous solution was monitored using a combination of HPLC and UV-visible absorption spectroscopy methods. Zeolite improves the photo-efficiency of titanium dioxide due to synergistic effects of the improved generation of active radicals ($S_2O_8^{2-}$ and OH*). Orange II underwent a further rapid degradation by the introduction of zeolite-TiO$_2$ due to strong adsorption and space effects. The degradation activity to Orange II follows the decreasing order: BDD-zeolite-TiO$_2$ > BDD > zeolite-TiO$_2$. The degradation rate was seen to increase with OH* radicals resulted from $S_2O_8^{2-}$ which produced on the BDD surface and by the zeolite-TiO$_2$ catalyst. Orange II could be almost completely degraded to CO$_2$ and H$_2$O after 180 min of electrolysis time by this joint treatment system.

1. INTRODUCTION

During the past decade, there have been a number of efforts on the degradation of organic pollutants in wastewaters from azo-dye industry. Even so, it is well known that complete degradation of dye-containing pollutants in wastewaters, which means the dyes are completely mineralized into CO$_2$ and H$_2$O, still presents a challenge for the wastewater treatment technology [1-3].

Among the current strategies for dye degradation in wastewaters, electrochemical oxidation (EO) has drawn interests since it has advantages such as powerful oxidation, easy for automation, and environmental-friendly [4-6]. Efficiency of the EO processes is found to depend on the anode material and the operating condition. Until now many types of electrodes have been employed in EO process and wastewater degradation industry. In recent years, electrochemical oxidation using boron-doped diamond (BDD) electrodes has been realized as one effective technology for the treatment of organic pollutants in industrial wastewaters [7-8]. BDD prepared by chemical vapor deposition (CVD) technology is an ideal electrode material with special advantages, which include high overpotentials, high chemical stability, and low background currents [9-10]. The most useful property of BDD electrodes in wastewater treatment is the ability for electro-generation of hydroxyl radicals (OH*) at high anodic potentials. OH* radical has a very high potential, only lower than fluorine. Therefore, OH* radicals have the ability to transform vast majority of organic compounds into CO_2 and H_2O [11]. This practical property makes BDD electrodes ideal candidates for wastewater treatments in the field of environmental protection.

Unfortunately, the electrochemical activity of BDD films decays very fast when extending into bulk electrolyte compared with that on BDD surfaces due to the limitation caused by mass transfer through diffusion process [7]. This limitation brings low current efficiency which makes oxidation on small or trace amounts of organic species in bulk solutions very difficult. Additionally, another major drawback of BDD electrochemical treatment is the high energy consumption to the mineralization of organics. Therefore, complete degradation of wastewater by BDD electrochemistry individually is very limited since it is unable to treat low-level or trace amounts of organics in bulk solutions. It necessary to address such kinds of problems for mineralization of azo dye wastewater in a wide range of concentrations.

Hence, introduction of certain catalysts in the electrical field combining with photochemical methods may overcome the disadvantages of BDD electrochemical oxidation and increase the treatment ability while decreasing the energy consumption [12]. Such a method, capable for wastewater purification, especially for a wide range of dye concentrations, is the heterogeneous photocatalysis in bulk solutions [13-14]. This kind of photocatalysis may be regarded as advanced oxidation process (AOP) in the supplementary treatment of wastewater by BDD electrochemistry [15]. In this case, combination of BDD electrochemistry and photocatalytic AOPs is expected to be a promising and attractive method for effective degradation of dyes in wastewaters.

In recent years, titanium dioxide (TiO_2) materials have been used in the photocatalytic degradation of organic pollutants [16]. TiO_2 photocatalysts can decompose many kinds of organic species even bacteria into CO_2 and H_2O with UV-vis light irradiation [17]. However, recovery and microfiltration processes are usually needed due to the small size of TiO_2 nanoparticles which bring complication of practical operations. Until now much efforts have been made to anchor TiO_2 on suitable substrates to improve its photocatalytic efficiency [18-19]. Currently the introduction of supporting matrix with micro or meso-pores (eg. zeolites) for TiO_2 nanoparticles has been realized as one promising method to increase the reactivity [20]. The advantages of zeolite-TiO_2 mainly includes: more adsorption sites and decreased scattering zones for UV light due to silica component in zeolites. Hydrophobic zeolites are excellent substrates for loading TiO_2 owing to the nano-scale channels and

cavities, high thermal stability, high chemical stability, and enhanced adsorption ability for target molecules [21-22]. In addition, zeolites can be used as matrices for photocatalysts that show good transparency to light illumination and high photochemical stability [23-24]. Moreover, zeolite is also used as a kind of Lewis acid catalyst, an adsorbent and an ion exchanger to improve TiO_2 catalytic efficiency [25].

Until now, even BDD-TiO_2 systems have been realized as promising technology in environmental protection field [5,17,26], some aspects on the joint effect deserve deep research. In the present study, a novel electrochemical-photocatalytic recycling system used for wastewater treatment with BDD electrodes and zeolite-TiO_2 catalyst is reported. This photocatalytically-assisted electrochemical system was applied to evaluate the treatment efficiency of Orange II degradation because the organic pollution caused by Orange II is of seriously environmental concern due to its high toxicity [2-3]. Furthermore, Orange II is a typical kind of azo-dye that is difficult to degraded by normal chemical and biological methods [6]. In this research Orange II was chosen as a representative model to investigate because it is one of the most difficult-to-remove pollutants in wastewater treatment industry. On the other hand, some mechanism about the generation of active radicals in the presence of zeolite-TiO_2 on UV illumination are worth discussing in this study.
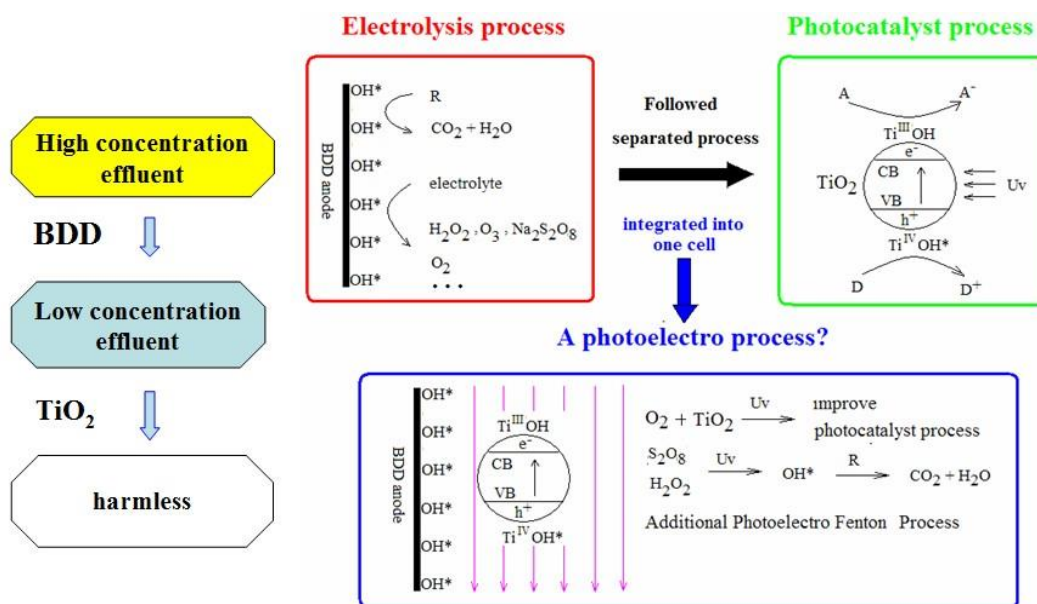
Scheme 1. Illustration for research of the synergistic degradation of wastewater which are composed of electrochemical and photocatalytic process. A hybrid process combined of electrochemical and photocatalytic treatment has enhanced effect for the degradation of Orange II.

As shown in Scheme 1, the investigation of photo-electro degradation to Orange II on BDD in relation to zeolite-TiO_2. One important objective of this study is the investigation of the mechanism of active radical generation for Orange II degradation on the BDD-zeolite-TiO_2 hybrid process. Until now, to our best knowledge, photo-electro activated degradation of pollutants in wastewaters on BDD-zeolite-TiO_2 systems has not been thoroughly investigated. Although there have been a number of like research articles [5,12,17,27,28], nearly none of them have involved a comprehensive study on the

generation of active radicals in the combined photo-electro process. In this work, zeolite was used as the TiO_2 support and an alternative method was proposed according to which zeolite particles covered with TiO_2 were embedded in the system for further degradation of the Orange II under UV light. In this treatment process, high-level Orange II solution was degraded to low concentration by BDD electrolysis. Meanwhile, the low-level Orange II in the bulk solution was further purified by photocatalysis on zeolite-TiO_2. In this case, a photo-electro Fenton-like process is built and is expected to break through the mass transfer limitation and the combination effect of these materials greatly enhanced the electro-photocatalytic decolorization of Orange dye solution. This novel approach may be extended for a wide range of dye wastewater treatment with high efficiencies.

2. EXPERIMENTAL

2.1 Materials

Orange II was reagent grade of Fluka product. The solutions were prepared using pure water from a Milli-Q generation machine (M-Q water, 18.2 MΩ cm). Na_2SO_4 and zeolite, of the purest available quality, were obtained from Wako. The sample solutions were prepared by dissolving Orange II in distilled water. Titanium tetrachloride ($TiCl_4$) was purchased from Aldrich. Zeolite (β type) were purchased from Fluka and used without any purification.

2.2 TiO_2 Coating on Zeolite

$Ti(OH)_4$ was firstly precipitated from diluted $TiCl_4$ aqueous solution by ammonium solution. Then the $Ti(OH)_4$ precipitation was washed 10 times with distilled water and a gel of $Ti(OH)_4$ was obtained. The zeolite balls in suspension were dipped into the $Ti(OH)_4$ solution for 12h. The $Ti(OH)_4$ coated zeolite balls were then calcinated at 450^oC for 6h. The amount of TiO_2 loading was about ~30%, which was estimated by the weight loss in calcination in an air stream at 500^oC for 5 h.

2.3 Design of the Photo-electro Cell

A schematic illustration of the working principle of the BDD-zeolite-TiO_2 system is showed in Scheme 2. The galvanostatic electrolysis was carried out in a photo-electro flow cell which was self-designed. In the center of the cylindrical reactor, a UV light source was mounted using a mercury vapor lamp with a wavelength of 365 nm. All experiments were carried out under constantly stirring at 200 rpm using a magnetic stirrer to make the catalyst good dispersion and to maximize the exposure of the catalyst to the UV light.

The electrochemical degradation was carried out using in a three-electrode cell (Scheme 2), which contained a BDD electrode serving as the anode and a Pt electrode used as the cathode. The geometric area of both BDD and Pt electrodes was 10×10 cm^2 with a gap of 10 mm. 0.1 M Na_2SO_4 solution was used as the electrolyte. The original concentration of Orange II in the cell was adjusted to

100 ppm in a total volume of 1 L. The solution flow was kept at 100 mL min^{-1} rate and the anode potential was set at 4.5 V (Vs. SCE). The electrolysis was run under continuous stirring condition. A regulated direct current (DC) power was supplied in the galvanotactic zone with a current density at 100 mA cm^{-2}. The high-level Orange II wastewater was passed through the BDD surface and circulated in the cell flow transferring into low-level solution. Meanwhile the low-level solution was treated by the photocatalysis in the circulation.
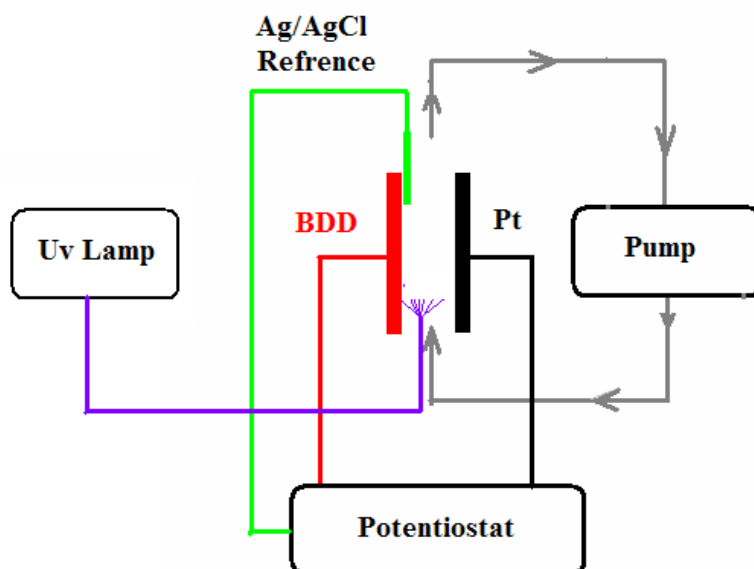
Scheme 2. Schematic illustration of the BDD-zeolite-TiO$_2$ system for Orange II degradation.

The catalytic activity was tested in the photo-assisted treatment of Orange II with Na$_2$SO$_4$ under UV light. The flow solution was circulated in the reaction cell through a peristaltic pump. The temperature of the reactor was controlled by a surrounded walled jacket with in-flowing water. The photocatalyst particles were introduced into the electrolyte by stirring dispersion at 40°C temperature in the photo-electro process. Orange II was photo-catalytically degraded in the suspension containing 1g L^{-1} photocatalyst.

The concentration of Orange II was monitored with an LC-2010CHT HPLC system (Shimadzu) with an Ultron VX-ODS column (Shinwa Chemical). A MeOH: H$_2$O (50:50) was used as the mobile phase with a0.5 mL min^{-1} flow rate. The column temperature was kept at 40°C. Samples of 20 μL each were periodically taken for HPLC analysis, again as the reaction occurred. A UV light source (FL10BLB, Toshiba) was employed for the measurements of the species. The concentration of Orange II in the degradation process was recorded with the UV-visible spectrophotometer and the results were obtained in 180 min treatment course. The absorbance of the Orange II solution at 484, 310 and 230 nm was measured by the UV-vis spectrometer. The products were identified by comparison with standard references.

3. RESULTS AND DISCUSSION

3.1. Orange II Removal in a Synergistic Process

The BDD, zeolite-TiO$_2$, BDD-zeolite-TiO$_2$ treatment efficiencies were compared by each electrochemical and photocatalysis result. The changes of the Orange II concentration were analyzed by UV$_{484}$ measurement versus time. As can be seen from Figure 1, noticeable enhancements in degradation efficiencies were obtained when combined with the zeolite substrates. After a reaction time of 180 min, about 6.5, 72.3, and 99.99% amount of Orange II was degraded in the photocatalysis (zeolite-TiO$_2$), electrooxidation (BDD), and photo-electro (BDD-zeolite-TiO$_2$) treatments. It should be noted that all the three times of removal efficiencies for Orange II, monitored by UV$_{484}$, increase with the time.
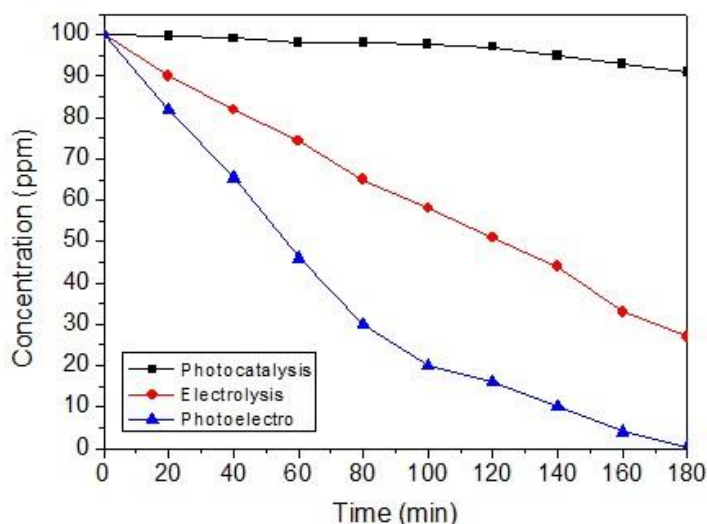

Figure 1. Comparison of the efficiency of the system for Orange II removal. Evolution of Orange II degradation versus the reaction time, expressed in terms of: red line: BDD electrochemistry with UV irradiation; black line: zeolite-TiO$_2$ electrolysis with UV irradiation; blue line: synergistic process on BDD-zeolite-TiO$_2$ treatment.

As observed in Figure 1, BDD in combination with zeolite-TiO$_2$, namely the photo-electrochemical process, exhibits the highest slope meaning the strongest degradation ability to Orange II. Obviously the BDD-zeolite-TiO$_2$ treatment has the best degradation activity, which may be due to a synergetic effect of the electrochemical and photocatalytic process. A powerful discoloration of Orange II on the BDD electrode but without zeolite-TiO$_2$ photocatalysis was clearly observed in the initial few minutes, and then became very slow. It is noticeable that the degradation by an individual photocatalysis to mass Orange II shows only a very slow decay in the Orange II concentration, indicating that a single photocatalytic treatment is unsuitable for high-concentration dyes. The significantly high discoloration efficiency to Orange II, which may be attributed to the synergetic effect of BDD and zeolite-TiO$_2$, is speculated to oxidize Orange II due to OH* radicals generating

from the electrolysis in the presence of Na_2SO_4 under UV light. In this combined treatment process, a lot of active OH* radicals are generated which have very high activity transforming organic compounds to CO_2 and H_2O.

3.2. Direct Electrochemical Treatment Process on BDD

The role of BDD is to generate OH* which directly oxidize Orange II. BDD exhibits a very high overpotential for both hydrogen and oxygen evolution compared with many traditional anodes. This advantage allows the easy generation of active hydroxyl (OH*) radicals by H_2O decomposition, according to the following reaction [7,8]:

$$H_2O \rightarrow OH^* + H^+ + e^- \qquad\qquad (1)$$

Orange II molecules that reach the BDD anodic surface can be directly oxidized by the electrogenerated OH* to H_2O and CO_2. Meanwhile on the BDD surface, peroxodisulfate ($S_2O_8^{2-}$) is also produced with a high current efficiency from a concentrated sulfate solution (Na_2SO_4). The produced oxidants (peroxodisulfate) subsequently diffuse into the bulk electrolyte and mix with the UV-lighted wastewater in order to achieve mass production of OH* radicals, which can decompose the organic species in wastewater. The following mechanism is proposed for photo or thermal decomposition of persulfate in aqueous solutions [11,29].

$$S_2O_8^{2-} + UV \rightarrow 2SO_4^-* \qquad\qquad (2)$$
$$SO_4^-* + H_2O \rightarrow HSO_4^- + OH^* \qquad\qquad (3)$$

In this case, complete decomposition of Orange II by OH* radicals as the oxidant is a main reaction, giving CO_2 and H_2O as the final products. Generally, the relationship between the organic concentration and the electrochemical reaction rates is expressed as a pseudo first-order equation [17]. The electrolysis treatment is especially able to reduce the high-level Orange II value to very low concentrations. The current efficiency is decreased after about 60 min in the electrochemical treatment. The degradation in the initial 60 min of the electrochemical reaction is enough for the representation of the whole treatment process.
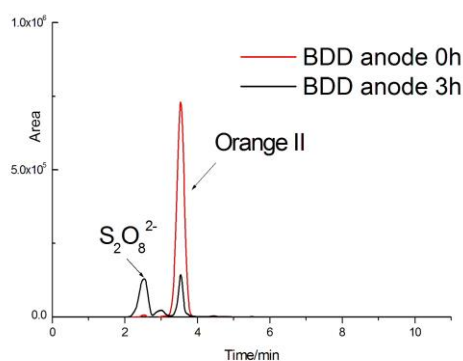

Figure 2. Typical HPLC result of Orange II electrolysis process. Mobile phase: MeOH:H_2O=50:50(v/v), iniection:20uL; analyses: ODS-2(5um), 40°C, detector wavelengths: 484nm, 310nm, 230nm.

HPLC analysis of the solution from Orange II degradation experiments revealed the presence of the key intermediate species. Comparison of the HPLC result at initial and after a period time is shown in Figure 2. The photoproducts from 0 to 10 min were chromatographically isolated and fully characterized by UV-vis analysis. It is observed that, during the degradation process, a sequence of new peaks ($S_2O_8^{2-}$) appeared and increased with increasing electrolysis time. After 2.5 min of eluent time, the solution released a large amount of $S_2O_8^{2-}$ ions. Meanwhile, the concentration of Orange II decreased about 80% according to the change of the feature peaks at 3.6 min. From the HPLC results it is clearly shown that BDD electrochemistry has a distinct advantage to treat dye wastewater in high-level concentrations.

As mentioned above, compared to photocatalytic methods, BDD is not suitable for the treatment of wastewaters especially at lower concentrations, indicating that a single electrochemical oxidation process is not efficient in complete degradation of dye wastewaters. Furthermore, it must be emphasized that electrochemical oxidation is not an economic technology since high energy consumption is needed. And the formation of OH* by electrochemistry requires high electric supply that may cause waste of energy and low efficiency of current. In the BDD electrochemical course, although the electrolysis is exceeding until the visible color is almost removed, past reports pointed out that electro treatment alone reaches an incomplete result, because potentially toxic aromatic amines are produced from azo dyes [6].
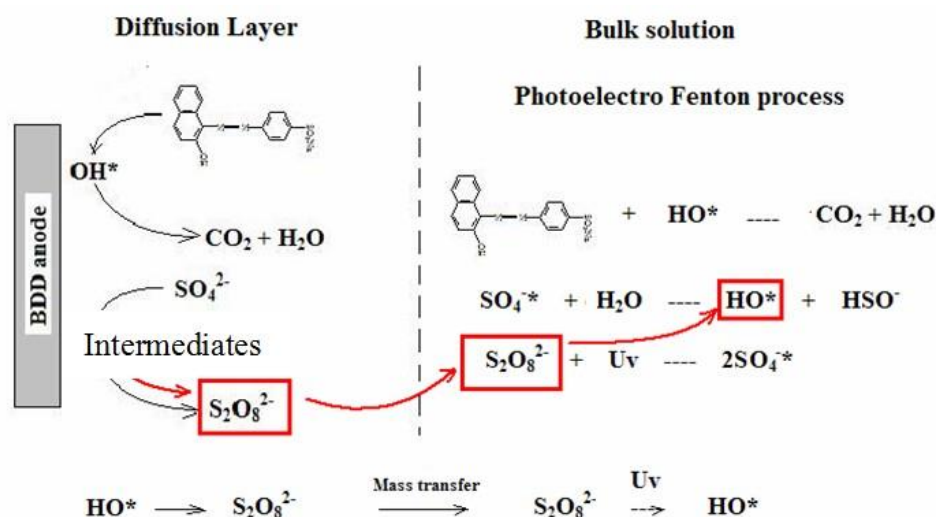

Figure 3. Schematic illustration of mass transfer limitation in the photo-electro process on BDD anode. In the diffusion layer on BDD surface, Orange II is oxidized into H_2O and CO_2 by the OH* that generated on the BDD anode, and SO_4^{2-} is transformed to $S_2O_8^{2-}$ under a high applied potential. However, only small amounts of $S_2O_8^{2-}$ radicals, which can transform H_2O to OH* under UV light, diffuse into the bulk solution because of the effect by mass transfer limitation,

In terms of electrochemical activity, significant influence of UV irradiation on the BDD electrolysis has been researched by Akira Fujishima [7]. It is well known that hydroxyl radicals are formed in a solution when hydrogen peroxide is mixed with ferrous ion (Fenton reactant), as well as when peroxodisulfate is mixed with silver ion or when a peroxodisulfate solution is heated or upon UV irradiation [1,30]. In this case, a homogeneous AOP process happens in the bulk solution as shown in

Figure 3. The role of the BDD electrode is transforming SO_4^{2-} to $S_2O_8^{2-}$ radicals which further react with H_2O under UV light, thus forming a chain of the photochemical AOP reactions. However, these separated radicals are quickly recombined if no stable reagents or conditions are afforded. This process is subject to mass transfer limitation, which means most of the active radicals are distinguished before they diffuse into the bulk solution. Since BDD electrochemistry consumes a large amount of electric power, this mass transfer limitation brings a great waste of energy and a low current efficiency. How to prolong the lifetime of the active radicals is a significant challenge. Hence, introduction of suitable catalysts in the bulk solution is necessary.

3.3. Influence of Zeolite

3.3.1. Orange II Removal on BDD-zeolite in Photo-electro Process

The system behavior was studied without/with light irradiation and in the absence/presence of the zeolite photocatalyst. The degradation of Orange II by BDD, zeolite, and BDD-zeolite under UV irradiation processes suggested that different degradation efficiencies and the results are compared in Figure 4. The pore size of the zeolite is slightly larger than the target molecules that they were going to adsorb, so they might allow passing into the microstructure of the zeolite [31]. The nanostructure of the added zeolite is regarded as an important factor in the promoted photo oxidation. In addition, introduction of the zeolite also increases the amount of the active radicals in the bulk solution since it prolongs the lifetime of the generated active radicals.
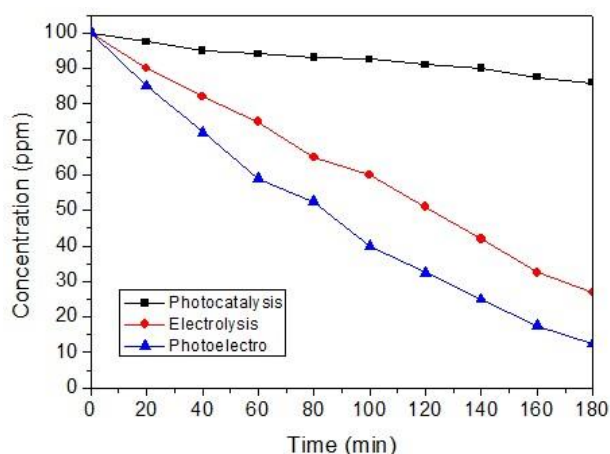

Figure 4. Orange II removal in the photo-electro process with BDD and zeolite. Black line: photocatalysis on zeolite under UV irradiation without BDD; red line: BDD electrolysis under UV irradiation without zeolite; blue line: treatment on BDD-zeolite photo-electro process.

Generally, the photocatalysis reaction kinetic can be described by the Langmuir-Hinshelwood model, which is expressed as a pseudo first-order equation. Nevertheless, the zeolite photo-electro process without the BDD electrolysis improves a little to the Orange II degradation as indicated in Figure 4. In the absence of the BDD electrodes, almost no difference between in the zeolite-filled cell

and in the empty cell was observed. As discussed above, in the BDD treatment for Orange II wastewater the generated OH* radicals are far below the levels on the BDD surface. To overcome such drawbacks, Efforts have been made to explore how to efficiently disperse OH* radicals into the homogeneous solution by the zeolite catalysis.

3.3.2 Dependence of UV Light and Zeolite for Peroxodisulfate Generation in Electro-photo Process

Zeolite materials can stabilize certain reactive intermediates formed in photochemical processes [32]. The mechanistic aspects relating to the generation of peroxodisulfate on BDD with UV light and in the presence of zeolite were investigated. As mentioned above, Peroxodisulfate is produced as an intermediate that plays an important role in the generation of hydrogen peroxide and zeolite influences the peroxide generation during the photo-electro process [8]. For comparison, a photo-catalytical process for Orange II degradation was performed in the same conditions with or without zeolite and the results are shown in Figure 5.
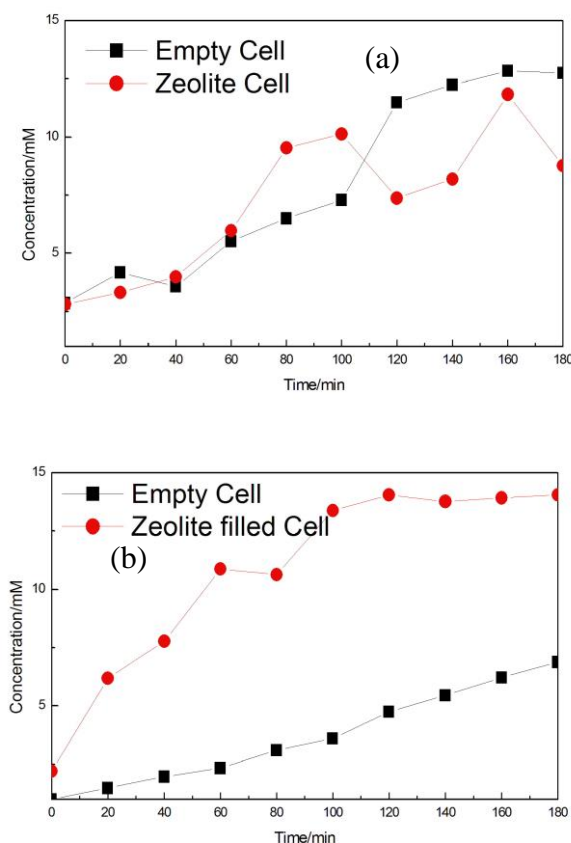

Figure 5. $S_2O_8^{2-}$ generation vs. photo-electro time (a) without UV illumination; (b) with UV illumination. Black line: BDD treatment without zeolite; red line: BDD treatment in a zeolite-filled cell.

In Figure 5, the generation of $S_2O_8^{2-}$ was compared between the empty and zeolite-filled cells to estimate the effect by the factors of zeolite and UV light. The results show that (1) $S_2O_8^{2-}$ concentration was almost the same without UV irradiation despite of the presence of zeolite in the electrolysis cell, no significant effect of the catalyst in the absence of UV irradiation was observed; (2)

$S_2O_8^{2-}$ concentration increased rapidly with UV irradiation in the zeolite-filled cell. After the reaction time of 180 min, about 7 and 13 mM of $S_2O_8^{2-}$ was generated on BDD and BDD-zeolite, respectively; (3) The $S_2O_8^{2-}$ production on BDD-zeolite, was initially rapid, over the first 2h, and then sloped gently.

Since the $S_2O_8^{2-}$ concentration showed almost no significant difference in the empty cell and zeolite-filled cell without UV irradiation, it should be noted that UV light is key factor in the generation of $S_2O_8^{2-}$, improving the generation rates of OH*. Without UV irradiation, zeolite shows almost no efficiency in the generation of $S_2O_8^{2-}$. This kind of photochemical reaction is confirmed increase the formation of $S_2O_8^{2}$ as a predominant intermediate by direct irradiation of SO_4^{2-} in zeolite as monitored by HPLC method.

3.3.3 Suggested Mechanism: A Photo-electro Fenton Process

The experimental results suggest that the promotion of the degradation reactivity is due principally to the catalysis from the Lewis acid site contents of zeolite. The amount of the Lewis acid zone is a key factor in the photocatalytic course [33-34]. As reported elsewhere, it is regarded that the hydrophobicity degree is in connection with the residual aluminum content in zeolite [23]. In addition, it is noteworthy that zeolite with high surface area and ring-pores structure, is preferably adsorb target molecules [32]. In addition, in comparison with other catalysts, zeolite has better ion-exchange capability in acidic media. In this photo-electro process we speculate that, in the acidic solution, aqueous SO_4^{2-} can interact with the surface hydroxyl groups of alumina on the acidic zeolite (zeolite-$(AlO)H^+$), leading to the continuous formation of $S_2O_8^{2-}$ radicals. The mechanism for this process has been proposed by Comninellis and involves intermediate formation of $SO_4^{-}*$ anion radicals, which then react with another $SO_4^{-}*$ in the electrolyte to produce an $S_2O_8^{2-}$ radicals [8]. It is then $S_2O_8^{2-}$ radicals decomposes H_2O molecules into OH* radicals under UV light.

In this photo-electro course $S_2O_8^{2-}$ radicals come mainly from two ways:

(a) Diffusion layer on BDD surface

$$SO_4^{2-} \rightarrow S_2O_8^{2-} \qquad\qquad (5)$$

(b) Bulk electrolyte

$$SO_4^{2-} + \text{zeolite-}(AlO)H^+ \rightarrow \text{zeolite-}(AlO)HOSO_3^- \qquad (6)$$

$$\text{zeolite-}(AlO)HOSO_3^- + OH* \rightarrow \text{zeolite-}(AlO) + SO_4^{-}* + H_2O \qquad (7)$$

$$2SO_4^{-}* \rightarrow S_2O_8^{2-} \qquad\qquad (8)$$

In the presence of zeolite, SO_4^{2-} in the bulk solution are attacked by OH* when they are anchored in the micropores with the H-O-zeolite bonds under the Lewis acid-base catalytic reactions. Hence, a large amount of $S_2O_8^{2-}$ radicals are continuously generated under the catalysis of zeolite. According to references [9, 35], $S_2O_8^{2-}$ radicals are generated from the reactions between HSO_4^- or molecular H_2SO_4 with OH* radicals, following the illustration as shown in Figure 6(a). As can be seen in Figure 6(a), in the allotropic forms of HSO_4^- and SO_4^{2-}, the coordination of S atom is fourfold with O atoms forming a distorted tetrahedron: the S atom is shared by three adjacent O atoms and one -OH group. The distortion of the tetrahedral in this phase leads to crystallographic differences and results in different arrangement of the S-O and S-OH bonds on the surface of the zeolite particles. The axial S-

OH bond with a 155pm length is longer than the four equatorial S-O bonds (144pm length) of SO_4^{2-}, which makes the distortion angle of 98° is possible to be attacked by OH* radicals to form S-O-O* (SO_4^-*). In this case, the zeolite-(AlO)$HOSO_3^-$ unit, with a similar structure of HSO_4^-, is formed by the reaction of SO_4^{2-} with a hydrogen atom from the acidic zeolite (zeolite-(AlO)H^+). It has been found that the aluminum sites and related cations can attract polar molecules through dipolar-dipolar or electrostatic interactions [23]. Based on the experimental results and literatures [36], we speculate an S-O-H bond is shared with a surface Al atom on the surface structure because HSO_4^- (zeolite-(AlO)$HOSO_3^-$) is more close to the oxygen atoms at Al than at Si sites. A hydrogen bond is then formed between the hydrogen atoms of HSO_4^- (zeolite-(AlO)$HOSO_3^-$) and the oxygen atoms of the negative charged framework. The neighboring Lewis groups in the structure play an important role in the photochemistry and the formed bond strength is in connection with the electron acceptance ability of the neighboring Al(IV) sites. With such an anchoring of HSO_4^--like structure to the zeolite-(AlO) framework, the active species SO_4^-* could be easily formed when attacked by the OH* radicals by breaking of the H-Al bond and the H-O bond. Furthermore, small amounts of HSO_4^- generated in Eq.(3) from BDD electrochemical process also participate in the SO_4^-* generation reaction.
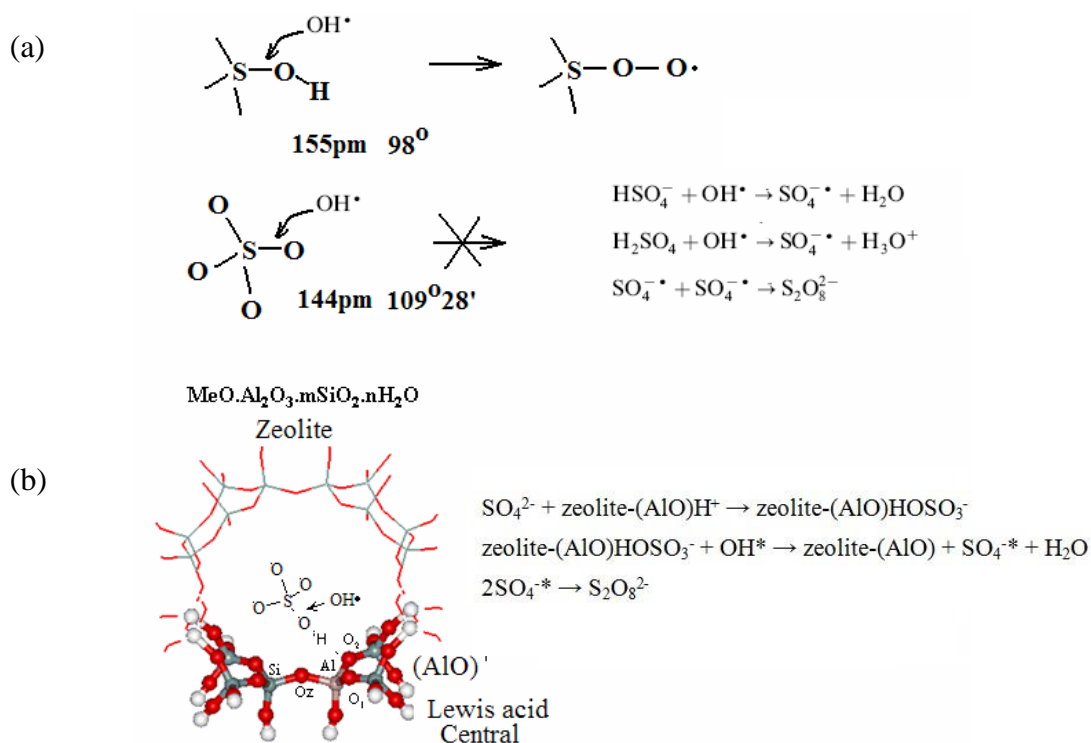

Figure 6. (a) Schematic illustration of the structures of HSO_4^- and SO_4^{2-} in $S_2O_8^{2-}$ generation reaction; (b) Structure of the adsorption complex of SO_4^- in the zeolite pore, and scheme for the catalytic process on zeolite in the generation of $S_2O_8^{2-}$.

The stoichiometry in Figure 6(b) clearly shows the possible increase of the amount of $S_2O_8^{2-}$ in the bulk electrolyte during the catalytic process of zeolite. Since sulfate radicals are formed via the reaction of HSO_4^- ions and molecular H_2SO_4 with OH* radicals, the absorbance of SO_4^{2-} and the lewis acid central in zeolite may form $_3$OS-O-H-zeolite lattice. Therefore, the formation of SO_4^-* and $S_2O_8^{2-}$

in a large amount is expected. By converting SO_4^{2-} radicals to $SO_4^{-}*$ substances, the amount of the active oxidant radicals ($S_2O_8^{2-}$ and OH*) is increased in the presence of the lattice of zeolite-$(AlO)HOSO_3^{-}$ unit and becomes high level in the bulk solution as well as that generated on the BDD electrode. Apparently, we observed a highest activity when using zeolite with large amount of Lewis sites.

As shown in Figure 7, both the OH* and $S_2O_8^{2-}$ life time are apparently prolonged in the presence of zeolite in the bulk solution. Therefore, the presence of SO_4^{2-} in the bulk electrolyte is necessary for the photochemical decomposition of Orange II catalyzed by zeolite. The nature of the SO_4^{2-}-zeolite interactions, for example, seems to have a significant effect on the generation of $S_2O_8^{2-}$. It is concluded that catalysis of zeolite gives rise to relatively long-lived free OH* radicals, and $S_2O_8^{2-}$ plays an important role in the synergistic system.
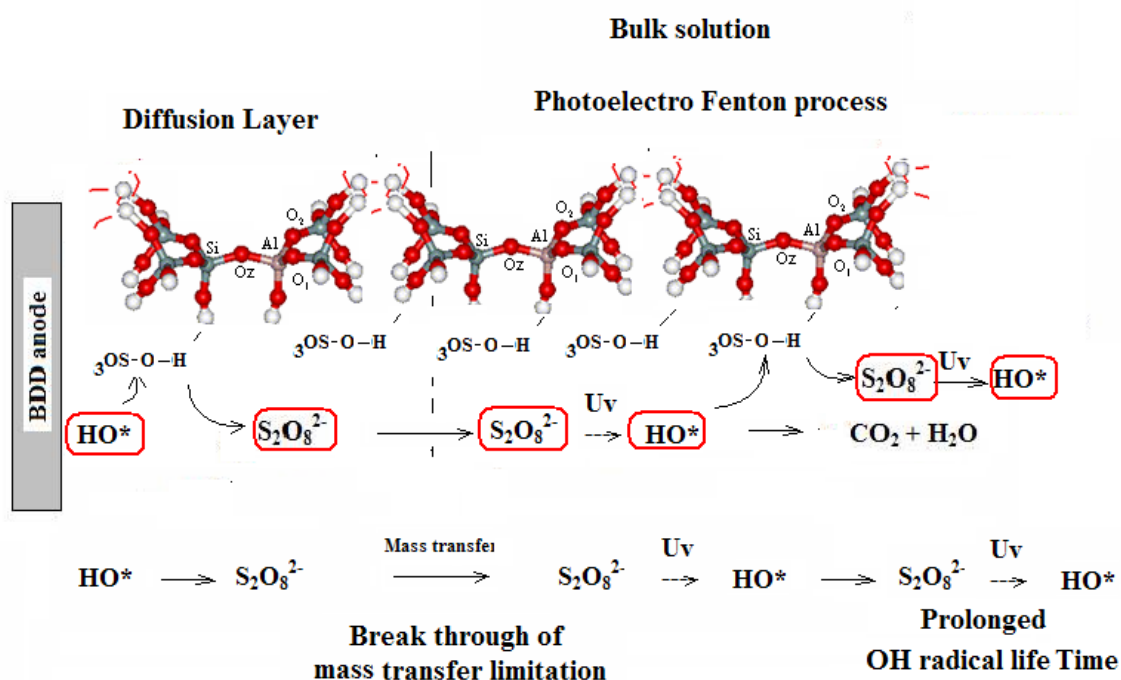

Figure 7. Scheme for the zeolite aided photo-electro process. SO_4^{2-} is converted to $S_2O_8^{2-}$ in the presence of zeolite, and $S_2O_8^{2-}$ further participates in a hydrolysis process under UV irradiation to generate OH*.

Figure 7 also presents the conceptual pathway of the breakthrough of drawback caused by mass transfer limitation. The most likely explanation, as discussed above, is that a constantly reciprocal generation of $S_2O_8^{2-}$ and OH* is proceeding on the BDD surface and maintained by the zeolite photocatalysis in the bulk solution. This photo-electro process means a ceaseless and mass production of hydroxyl radicals is constantly kept wherever in the diffusion layer or in the bulk solution. The mass transfer limitation, at least in a microscopical view, is diminished to a least extent. In this case, an enhanced efficiency is achieved for the degradation of Orange II due to the synergetic effect.

3.4. Influence of TiO₂ Addition

3.4.1. Synergistic Influence: TiO₂ Photocatalyst and Fenton Process

Introduction of zeolite decreased the effect of mass transfer limitation, and then introduction of TiO_2 led to a further improvement in the degradation efficiency. TiO_2 photochemical technology, as well as BDD electrochemistry, may be considered as an alternative method for environmental administration. For comparison, the photocatalysts were used in the same amounts with the same UV source. The experimental results disclose that the Orange II concentration, in comparison with the effect on solitary zeolite catalysis, was decreased around 10% when TiO_2 was loaded on zeolite (Figure 1 and 4). An enhanced effect on the degradation rate of Orange II is observed, which is due to more OH* radicals produced in the electrolysis cell. When Orange II is well adsorbed on zeolite support, it can be easily attacked by the nearby OH* radicals produced from the zeolite-TiO_2 interface. Furthermore, the intermediates formed in the degradation process are adsorbed on the zeolite, which also favors the complete mineralization of Orange II [32].

In order to gain more information of the effect from zeolite-TiO_2 on the degradation efficiency, generation of $S_2O_8^{2-}$ rate measured by zeolite and zeolite-TiO_2 under UV irradiation courses were plotted against time as shown in Figure 8.
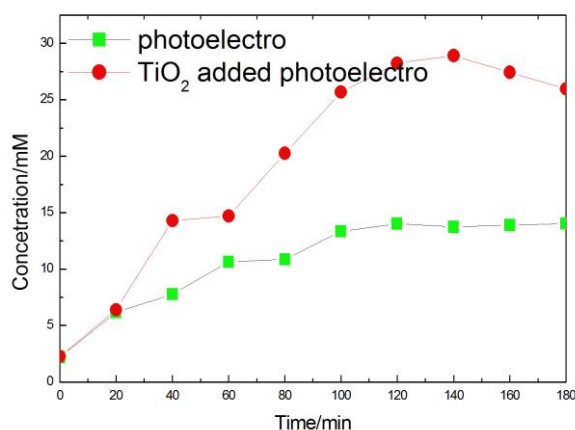

Figure 8. $S_2O_8^{2-}$ generation versus photo-electro time. Green line: photo-electro process on BDD-zeolite; red line: photo-electro process on BDD-zeolite-TiO_2.

The resulting catalyst significantly increased $S_2O_8^{2-}$ concentration from 2.5 to 28 mM while 2.5 to 13 mM within 180 min on zeolite as indicated in Figure 8. Based on the experimental results from Figure 1, 5, 8 and those reported elsewhere [37], we can conclude: (1) An enhanced generation of $S_2O_8^{2-}$ is observed on the zeolite-TiO_2 catalyst, which leads to the generation of more OH* under UV irradiation. (2) A Fenton-like AOP process may proceed on the zeolite-TiO_2 catalyst that plays an important role in the degradation of low-level dye in bulk solutions. Therefore, this results in the enhancement of the generation rate on supported TiO_2 catalysts. Thus, the zeolite-TiO_2 shows advantageous features compared with the original zeolite particles.

3.4.2. Proposed Mechanisms: More OH* Generation

As can be referenced elsewhere,[13] proper additives greatly influence the photoreaction of the organic species. The species such as H_2O_2 and $S_2O_8^{2-}$ in the solution can serve as as oxidants and reactions are described as follows:

$$S_2O_8^{2-} + Ti^{IV}OH \rightarrow SO_4^{2-} + SO_4*^- \qquad (9)$$
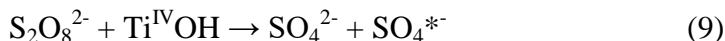$$SO_4*^- + H_2O \rightarrow SO_4^{2-} + OH* + H^+ \qquad (10)$$

Figure 9 may generally describe the photolysis of the zeolite-TiO$_2$, the subsequent transformation of $S_2O_8^{2-}$, the breakthrough of mass transfer limitation of $S_2O_8^{2-}$, and the transformation of $S_2O_8^{2-}$ to OH*. Obviously, the photocatalytic strength is correlated to the conversion of $S_2O_8^{2-}$ to OH*. It has been realized that the quantum yield of conventional TiO$_2$ photocatalysis is not high (less than 10%) because of the rapid recombination of the photo-generated charge carriers [38], which is an unfavorable factor in photocatalysis as well as energy waste. A high-level separation of the electron-hole pairs may be realized by using the zeolite-TiO$_2$ catalyst, on which OH* generation from $S_2O_8^{2-}$ in a chain style favors extending the lifetime of active radicals. Combining the experimental data with mechanisms proposed by the literatures [39], the high oxidation activity of BDD-zeolite-TiO$_2$ could be, at least partly, attributed to the two-way catalytic mechanism involving the Na$_2$SO$_4$/Na$_2$S$_2$O$_8$ redox couples. In addition, the application of an electric field produced by BDD could promote the separation of photo-generated electrons and holes [40] The sequence of degradation efficiency is BDD-zeolite-TiO$_2$ > BDD > TiO$_2$, which is of high consistence with the ability for the generation of hydroxyl radicals and $S_2O_8^{2-}$ on these substrates.
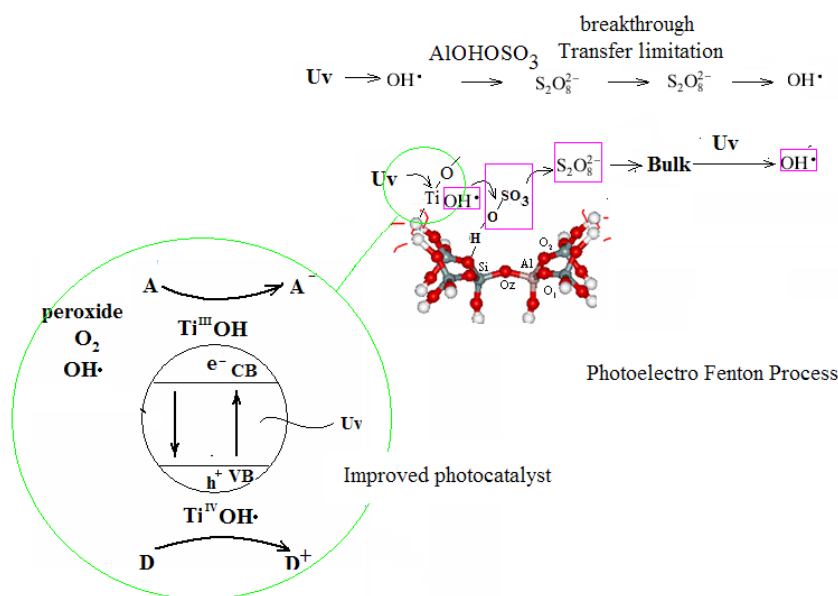

Figure 9. Schematic diagram of the proposed mechanism for the treatment of Orange II by photocatalysis on the zeolite-TiO$_2$ surface.

The charge carrier pairs are photo-generated when the zeolite-TiO$_2$ catalyst is illuminated by UV light with photo energy higher than 400 nm and the generation of electron-hole pairs takes place.

The photo-generated holes and electrons can decompose organic species in electrolyte due to a highly active potential. Hydrogen peroxide and hydroxyl radicals can be generated in this cell. When TiO_2 is loaded on zeolite, the photo-induced electrons at the interfacial zone transfer from the titanium on the zeolite to the enclosed HSO_4^- (zeolite-$(AlO)HOSO_3^-$) in a very short distance, immediately followed by breaking the $HO-SO_3$ bond to form $S_2O_8^{2-}$ radicals. In other words, the formation of the photo-produced OH* can be simply achieved as derived from an initial SO_3-O bond breaking of a SO_4^{2-} with the generation of A^- and D^+ pairs immediately from the TiO_2. Compared with zeolite catalyst, zeolite-TiO_2 catalyst exhibits a much higher velocity for the generation of $S_2O_8^{2-}$ and OH* radicals. This improvement due to the synergistic effect of the catalytic activity is like that of light-absorbing organisms of plant [41]. Furthermore, when illuminated by UV irradiation, the excited electrons from the conduction band of zeolite-TiO_2 take pathways very quickly from TiO_2 before the electron-hole recombination, because the zeolite surface with rich electron can serve as a hole scavenger [42-43].

The results indicated that this TiO_2-immobilized zeolite catalyst can effectively accelerate the minimization of dyes in wastewater, following the adsorption-decomposition and quick-space-charge-transfer mechanisms. This enhanced degradation can be attributed to two factors: adsorption and three-dimensional effect by the zeolite-TiO_2. In addition, TiO_2 encapsulated in zeolite with high area can expose a large number of active sites in the photochemical process [21]. Hence, zeolite-TiO_2 can serve as an efficient catalyst with low-cost for the application in the degradation of dye wastewaters.

We assume the drawback caused by the mass transfer limitation from BDD electrochemistry could be further eliminated upon the addition of zeolite-TiO_2 in the bulk electrolyte with Na_2SO_4 under UV irradiation. In other words, the generation of $S_2O_8^{2-}$ in the bulk solution is almost independent on BDD electrochemistry. For low amounts of Orange II in the wastewater, the photocatalytic process by zeolite-TiO_2 dominates the overall kinetics [44], which partly avoids the defect from the mass transfer limitation of electrochemical treatment. In this study, TiO_2 loaded zeolite in the presence of BDD electrochemistry showed a very high photoactivity to Orange II in aqueous media through the transportation of long-lived $S_2O_8^{2-}$ active species, unlike the results reported by other literatures that photo-activity of TiO_2 supported on those high-silica zeolite materials [45].

Comparisons with the other mainstream technologies are briefly summarized in Table 1. The advantage and disadvantage of this BDD-zeolite-TiO_2 system could be clearly indicated.

Table 1. Comparison the Orange II degradation method

Method	Orange II concentration	Degradation efficiency	Recycling operation	Energy consumption
Photocatalysis [46-48]	Low	70%~99%	Normal	Low
Electrochemistry [49-51]	High	> 90%	Good	High
BDD-zeolite-TiO_2	Very high	> 90%	Good	High

On the other hand, even the photocatalysis consumed relatively low energy, the photocatalytic process could not completely degrade high-level Orange II. In the aqueous solution Orange II is difficult to fully contact the surface of dispersed TiO_2 photocatalyst. Therefore, how to increase the mass transfer ability plays an important role in the industrial application of TiO_2 [24]. in this case, zeolite can be utilized as an Orange II adsorbent to enhance the photocatalytic activity. The proposed BDD-zeolite-TiO_2 system is an ideal strategy for high-efficient treatment of wastewaters.

4. CONCLUSIONS

The application of photocatalysis using zeolite-TiO_2 in wastewater electrochemical degradation by BDD exhibited an enhanced effect in Na_2SO_4 electrolyte. Orange II was chosen to evaluate the efficiency of this photo-electro degradation system. The Lewis acid sites of zeolite contributed from the fourfold coordinated aluminum play an important role in the photocatalytic reaction. These active sites could anchor SO_4^{2-} by one atom to the photocatalyst surface, and the connection is formed by sharing one oxygen-hydrogen bonding with a tetrahedral aluminum of zeolite through a coordinately unsaturated site. In terms of the apparent rate of Orange II degradation, mass transfer limitation of BDD electrochemistry was diminished in the presence of zeolite and Na_2SO_4 in the bulk electrolyte. The combination of BDD, zeolite, and TiO_2 allows for degradation of azo dye wastewaters more activity compared with electrochemistry and photocatalysis oxidation individually. This novel BDD-zeolite-TiO_2 system may have potential application in advanced oxidation process and industrial treatments of wastewaters.

References

1. H. Kusic, I. Peternel, S. Ukic, N. Koprivanac, T. Bolanca, S. Papic and A. L. Bozic, *Chem. Eng. J.*, 172 (2011), 109.
2. I. I. Raffainer and P. R. von Rohr, *Ind. Eng. Chem. Res.*, 40 (2001), 1083.
3. L. C. Abbott, S. N. Batchelor, J. R. L. Smith and J. N. Moore, *J. Phys. Chem. A*, 113(2009), 6091.
4. C. Y. Zhang, J. L. Wang, T. Murakami, A. Fujishima, D. G. Fu and Z. Z. Gu, *J. Electroanal. Chem.*, 638 (2010), 91.
5. C. Ratiu, F. Manea, C. Lazau, I. Grozescu, C. Radovan and J. Schoonman, *Desalination*, 260 (2010), 51.
6. J. Hastie, D. Bejan, M. Teutli-León and N. J. Bunce, *Ind. Eng. Chem. Res.*, 45 (2006), 4898.

7. A. Fujishima, Y. Einaga, T. N. Rao, and D. A.Tryk, *Diamond Electrochemistry*, (2005) Amsterdam, Netherland.
8. P.-A. Michaud, E. Mahé, W. Haenni, A. Perret and C. Comninellis, *Electrochem. Solid St.*, 3 (2000), 77.
9. K. Serrano, P. A. Michaud, C. Comninellis and A. Savall, *Electrochim. Acta*, 48 (2002), 431.
10. D. B. Luo, K. Nakata, A. Fujishima and S. H. Liu, *J. Photochem. Photobio. C: Photochem Rev.*, 31 (2017), 139.
11. S. Ahmed, M. G. Rasul, R. Brown and M. A. Hashib, *J. Environ. Manage.*, 92 (2011), 311.
12. Y. N. Hou, J. H. Qu, X. Zhao, P. J. Lei, D. J. Wan and C. P. Huang, *Sci. Total Environ.*, 407 (2009), 2431.
13. K. Rajeshwar, M. E. Osugi, W. Chanmanee, C. R. Chenthamarakshan, M. V. B. Zanoni, P. Kajitvichyanukul and R. Krishnan-Ayer, *J Photoch. Photobio. C: Photochem. Rev.*, 9 (2008), 171.
14. J. H. Ramirez, F. J. Maldonado-Hódar, A. F. Pérez-Cadenas, C. Moreno-Castilla, C. A. Costa and L. M. Madeira, *Appl. Catal. B: Environ.*, 75 (2007), 312.
15. G. T. Li, J. H. Qu, X. W. Zhang, H. J. Liu and H. N. Liu, *J. Mol. Catal. A: Chem.*, 259 (2006), 238.
16. L. Lucarelli, V. Nadtochenko and J. Kiwi, *Langmuir*, 16 (2000), 1102.
17. T. Ochiai, K. Nakata, T. Murakami, A. Fujishima, Y. Y. Yao, D. A. Tryk and Y. Kubota, *Water Res.*, 44 (2010), 904.
18. S. Fukahori, H. Ichiura, T. Kitaoka and H. Tanaka, *Environ. Sci. Technol.*, 37 (2003), 1048.
19. T. Kamegawa, R. Kido, D. Yamahana and H. Yamashita, *Micropor. Mesopor. Mat.*, 165 (2013), 142.
20. H. Yahiro, T. Miyamoto, N. Watanabe and H. Yamaura, *Catal. Today*, 120 (2007), 158.
21. S. Anandan, and M. Yoon, *J. Photochem. Photobio. C: Photochem Rev.*, 4 (2003), 5.
22. A. Bhattacharyya, S. Kawi and M. B. Ray, *Catal. Today*, 98 (2004), 431.
23. Y. Kuwahara, J. Aoyama, K. Miyakubo, T. Eguchi, T. Kamegawa, K. Mori, H. Yamashita, *J. Catal.*, 285 (2012), 223.
24. E. P. Reddy, L. Davydov and P. Smirniotis, *Appl. Catal. B: Environ.*, 42 (2003), 1.
25. J. Chen, L. Eberlein and C. H. Langford, *J Photoch. Photobio. A: Chem.*, 148 (2002), 183.
26. J. J. Yuan, H. D. Li, Q. L. Wang, S. H. Cheng and X. K. Zhang, *Mater. Technol.*, 30 (2015), 101.
27. C. Ratiu, F. Manea, C. Lazau, C. Orha, G. Burtica, I. Grozescu and J. Schoonman, *Chem. Pap.*, 65 (2011), 289.
28. J. J. Yuan, H. D. Li, Q. L. Wang, S. H. Cheng, X. K. Zhang, H. J. Yu, X. R. Zhu and Y. M. Xie, *Chem. Res. Chin. Univ.*, 30 (2014), 18.
29. I. M. Kolthoff and I. K. Miller, *J. Am. Chem. Soc.*, 73 (1951), 3055.
30. J. H. Ramirez, C. A. Costa, L. M. Madeira, G. Mata, M. A. Vicente, M. L. Rojas-Cervantes, A. J. López-Peinada ans R. M. Martín-Aranda, *Appl. Catal. B: Environ.*, 71 (2007), 44.
31. D. J. Doocey and P. N. Sharratt, *Process Saf. Environ.*, 82 (2004), 352.
32. M. V. Shankar, S. Anandan, N. Venkatachalam, B. Abrabindoo and V. Murugesan, *Chemosphere*, 63 (2006), 1014.
33. Y. Isaev and J. J. Fripiat, *J. Catal.*, 182 (1999), 257.
34. M. L. Guzmán-Castillo, E. López-Salinas, J. J. Fripiat, J. Sánchez-Valente, F. Hernández-Beltrán, A. Rodríguez-Hernández, J. Navarrete-Bolaños, *J. Catal.*, 220 (2003), 317.
35. M. Selvaraj, P. K. Sinha and A. Pandurangan, *Micropor. Mesopor. Mat.*, 70 (2004), 81.
36. N. Jiang, S. P. Yuan, J. G. Wang, H. J. Jiao, Z. F. Qin and Y.-W. Li, *J. Mol. Catal. A: Chem.*, 220 (2004), 221.
37. W. Panpa, P. Sujaridworakun and S. Jinawath, *Appl. Catal. B: Environ.*, 80 (2008), 271.
38. U. G. Akpan and B. H. Hameed, *J. Hazard Mater.*, 170 (2009), 520.
39. Y. J. Li and W. Chen, *Catal. Sci. Technol.*, 1 (2011), 802.
40. T. Spătaru, M. Marcu and N. Spătaru, *Appl. Surf. Sci.*, 269 (2013), 171.
41. M. J. Yoon, J. A. Chang, Y. H. Kim and J. R. Choi, *J. Phys. Chem. B*, 105 (2001), 2539.
42. M. Anpo, H. Yamshita, Y. Ichihashi, Y. Fujii and M. Honda, *J. Phys. Chem. B*, 101 (1997), 2632.

43. U. Bach, D. Lupo, P. Comte, J. E. Moser, F. Weissortel, J. Salbeck, H. Spreitzer and M. Grätzel, *Nature*, 395 (1998), 583.
44. H. Yamashita, S. Kawasaki, S. Yuan, K. Maekawa, M. Anpo and M. Matsumura, *Catal. Today*, 126 (2007), 375.
45. Y. M. Xu and C. H. Langford, *J. Phys. Chem. B*, 101 (1997), 3115.
46. F. Z. Li, G. T. Li and X. W. Zhang, *J. Environ Sci.*, 26 (2014) 708.
47. M. Mollah, A. Yousuf, J. A. G. Gomes, K. K. Das and D. L. Cocke, *J. Hazard. Mater.*, 174 (2010) 851.
48. L. Yue, J. B. Guo, J. L. Yang, J. Lian, X. Luo, X. N. Wang, K. H. Wang and L. Wang, *J. Ind. Eng. Chem.*, 20 (2014) 752.
49. J. Wang, C. Liu, L. Tong, J. S. Li, R. Luo, J. W. Qi, Y. Li and L. J. Wang, *RSC Adv.*, 5 (2015) 69593.
50. L. Cai, X.L. Xiong, N. G. Liang and Q. Y. Long, *Appl. Surf. Sci.*, 353 (2015) 939.
51. Y. J. Yao, F. Lu, Y. P. Zhu, F. Y. Wei, X. T. Liu, C. Lian and S. B. Wang, *J. Hazard. Mater.*, 297 (2015) 224.